

# SENZORI DE MONITORIZARE A COROZIUNII STRUCTURILOR DIN BETON ARMAT PRIN APLICAREA TEHNICII UNDELOR GALVANO-STATICE

## CORROSION MONITORING SENSOR IN CONCRETE STRUCTURES BASED ON THE GALVANO-STATIC PULSE TECHNIQUE

LU SHUANG\*, WANG ZHENG

<sup>1</sup>School of Architecture, Harbin Institute of Technology, Harbin 150001, China

*On-site corrosion sensor was developed to monitor the adverse effects in the chloride – contaminated concrete structures. Galvano-static Pulse Technique(GPT) was applied to measure the polarization resistance of the anodes and the electrical resistance of the surrounded concrete using the sensor. This paper presents the analysis of GPT measurements performed in the chloride-contaminated concrete for the laboratory tests. The relationship between the corrosion rate of steel electrodes and surrounded concrete resistance measured by corrosion sensor confirms the reliability of developed corrosion sensor. The results further show that the concrete resistance is also an indicative parameter which is related to the corrosion state of concrete structures.*

*Senzorii de coroziune montați in-situ au fost dezvoltati pentru a monitoriza efectele coroziunii datorată clorurilor asupra structurilor din beton. Tehnica undelor galvano-statice (GPT) a fost aplicată pentru a măsura rezistența de polarizare la anod și rezistența electrică a betonului prin utilizarea de senzori. Lucrarea prezintă analiza unor măsurători ale GPT efectuate asupra unor probe de laborator din beton contaminat cu cloruri. Relația între viteza de coroziune a oțelului electrozilor și rezistența betonului măsurată cu ajutorul unor senzori de coroziune confirmă încrederea în metoda senzorilor de coroziune. Rezultatele obținute indică faptul că rezistența electrică a betonului reprezintă un parametru influențat de starea de coroziune a structurilor din beton.*

**Keywords:** corrosion monitoring, concrete structures, GPT, polarization resistance

### 1. Introduction

Nowadays, structural deterioration in the concrete structures, mainly resulting from the corrosion of reinforcement, is a major concern for safety, economy and durability. Therefore, worldwide efforts were made to develop accurate corrosion monitoring technologies and effective corrosion sensors, in order to ensure a longer lifetime to concrete structures at the lowest life-cycle cost and to plan proper maintenance [1,2]. However, it should be noted that all methods from the previous experiments have their own disadvantages when they were used for on-site measurements [3,4]. The reasons are varied, but usually the methods mentioned above are time-dependent and can be disturbed by electro telluric currents or human factors. There has been a turning point in monitoring methodologies in accordance with the advent of Galvano-static Pulse Technique (GPT) [5].

During the past decade, a lot of efforts were being spent on improving this method. One of the major improvements is to confine the reinforcement area affected by the electrical signal using a guard ring counter electrode [6]. But unfortunately such guard ring system is found to be less effective in the following situations: (i) In highest point of portal frame in framed structures, columns and beams

located at elevated height, (ii) In bridge structure where one traffic lane has to be closed for a certain time, (iii) In concrete surface coated with an insulating paint [7]. Embeddable sensor is a viable method in such situations where the arrangement of the conventional surface-mounted probe cannot be used. Consequently, an embeddable Corrosion Monitoring Sensor (CMS) based on the GPT has been developed in this paper. The approach of the present investigation is to measure the polarization resistance ( $R_p$ ) of the rebar and the coverconcrete resistance ( $R_s$ ) of the surrounded coverconcrete using the CMS system and further to compare the measured values in chloride-contaminated concrete under the laboratory condition.

### 2. Experimental. Materials, Sensors and method of measurement

#### 2.1. Materials

P-O 42.5 cement used was from Harbin Cement Factory. The river sand was with a fineness modulus of 2.4 and the coarse aggregate was with a maximum size of 10 mm. To evaluate the electrical resistance and the corrosion rate measured by the CMS in the chloride-contaminated concrete, different cement chloride content was obtained by dissolving NaCl in water. The concrete proportioning is shown in Table 1.

\* Autor corespondent/Corresponding author,  
Tel.: +86 13214600050, e-mail: [hitlu@126.com](mailto:hitlu@126.com)

Table 1

| Mix proportion of the chloride-contaminated concrete / <i>Compoziția betonului contaminat cu cloruri</i> |   |   |   |  |  |             |
|--|---|---|---|--|--|-------------|
| NO. Nr.  | Cement contents<br><i>Dozaj ciment</i><br>[kg·m <sup>-3</sup> ] | Sand<br><i>Nisip</i><br>[kg·m <sup>-3</sup> ] | Coarse aggregate<br><i>Agregate mari</i><br>[kg·m <sup>-3</sup> ] | Water/cement<br>Ratio<br><i>Raport apă / ciment</i><br>[w/c] | Water<br><i>Apă</i><br>[kg·m <sup>-3</sup> ] | NaCl<br>[%] |
| A  | 358   | 714   | 1174  | 0.42   | 150  | 0           |
| B  | 358   | 714   | 1174  | 0.42   | 150  | 0.3         |
| C  | 358   | 714   | 1174  | 0.42   | 150  | 3.0         |

## 2.2. Sensor Arrangements

A typical layout of the CMS is shown in Fig. 1. Each anode ( $\Phi$  0.7 cm x 5 cm, Q 235 steel) spaced 2 cm from each other was fixed on a nylon frame. The bottom of the frame contained a built-in RE which can be found in previous paper [8]. And the apparent potential of the RE is about -40 mV vs. Saturated Calomel Electrode (SCE). To evaluate the correlation between sensor output and corrosion state of the sensor and surrounded concrete environment, each CMS sensor system was vertically embedded in the middle of the concrete cubic specimen (10 cm x 10 cm x 10 cm) as shown in Figure 2.

The depth between the top end of the CMS and the exposure surface of the concrete was 0.5 cm. The concrete specimens were cured under an ambient temperature of  $20\pm 1^\circ\text{C}$  and RH of 95% condition. All the electrochemical tests were conducted under the same condition.

## 2.3. Galvanostatic Pulse Technique Theory

The equivalent circuit shown in Figure 3 was usually used to interpret the electrical signal response of the Anode-Concrete system quantitatively. As shown in the figure  $R_p$  is the polarization resistance of the anode,  $C_{dl}$  is the double layer capacitance, and  $R_s$  is the concrete resistance. Typical potential transient response of CMS is shown in Figure 4.

An anodic current pulse  $I_{app}$  is impressed to the middle working anode ( $A_2$  or  $A_5$  in Fig.2) from two adjacent anodes ( $A_1$  and  $A_3$  electrodes refer to  $A_2$  in Fig.2) that act as the counter electrodes. The initial applied current  $I_{app1}$  is 500  $\mu\text{A}$  and the duration of the typical pulse is 10 seconds. When the constant current  $I_{app1}$  is applied to the system, the polarized potential of reinforcement  $E_t$  can be expressed as a function of polarization time:

$$E_t = I_{app} \left[ R_p \left( 1 - \exp \left( -\frac{t}{R_p \times C_{dl}} \right) \right) + R_s \right] \quad (1)$$

In order to obtain values of  $R_p$  and  $C_{dl}$ , Generally, the voltage across the  $C_{dl}$  element may keep constant under the step current (from  $I_{app1}$  to  $I_{app2}$ ) excitation, and thus the initial voltage drop  $\Delta E_1$  can be totally attributed to the concrete resistance  $R_s$ :

$$\Delta E_1 = E_1 - E_2 = R_s (I_{app1} - I_{app2}) = R_s \times I_{app1} \quad (2)$$

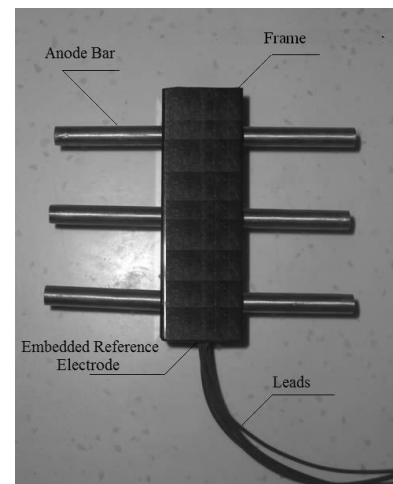
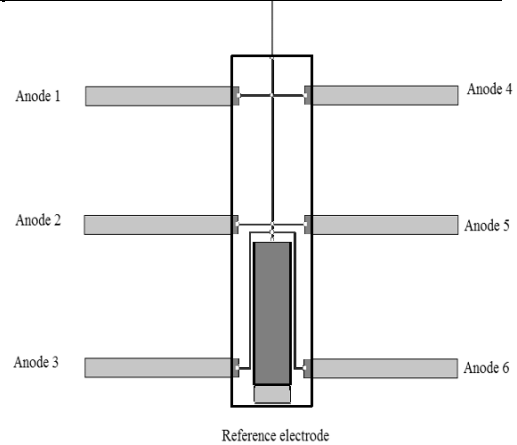


Fig.1 - Typical layout and picture of the CMS system  
*Schema tipică și fotografia sistemului CMS.*

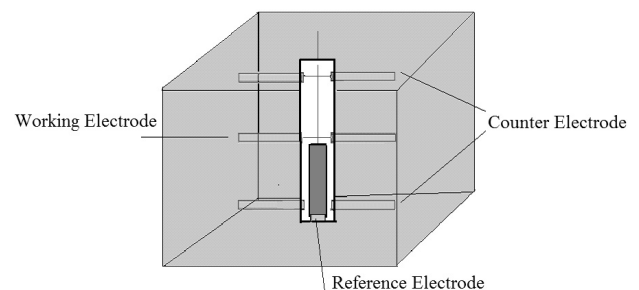


Fig. 2 - Configuration of the Sensor system in concrete specimens / *Configurația sistemului de senzori în probele de beton.*

As a sudden breaking current is adopted, corresponding to  $I_{app2}=0$  here, the applied current continuously flows out of the double-layer capacitance and the voltage across the  $C_{dl}$  element decreases by degrees. In the end, the voltage reaches a stable value as follows:

$$\Delta E_2 = E_1 - E_3 = I_{app1}(R_s + R_p) \quad (3)$$

In the equation, the remaining overpotential  $\Delta E_1$  and  $\Delta E_2$  which are the ohmic drop. Normally, the establishment of the linear polarization resistance  $R_p$  requires that  $\Delta E_2$  should not exceed 10 mV. Otherwise, the measured voltage will not show linear relationships with the applied current. After the value of ohmic drop is determined by means of this analysis, the  $R_s$  and  $R_p$  can be obtained from equation (2) and (3).

### 2.4 Electrochemical test

All the electrochemical measurements were performed by RST5200 electrochemical system. For each mix proportion (A to C), all the electrochemical parameters were measured six times and the result in the paper was an average value of six measurements.

#### 2.4.1. Potential test

Figure 5 shows the typical layout for electrochemical measurements of Potential of anodes vs. the reference electrode. The potential between the two single anodes ( $A_2$  and  $A_5$ ) in the different concrete and the accompanying reference electrode have been recorded at 30 seconds after coupling. The anode was connected to the working electrode terminal, and the build-in RE was connected to the reference electrode terminal.

#### 2.4.2. Concrete resistance and polarization resistance test

In addition, polarization resistance and the depth-related concrete resistance surrounded the anode bars was estimated according to the GPT method mentioned above as well. The response of embedded anode bars in contact with the concrete is represented by a simple circuit made up of the concrete resistance  $R_s$  ( $\Omega$ ) in series with a parallel Resistance-Capacitance (R-C) branch as shown in Fig. 3. Electrode configuration was exactly the same as the potential tests. The  $A_2$  or  $A_5$  was connected to the working electrode terminal, and it's worth noting that because the measurement configurations are used as two electrode pairs, the anodes ( $A_1$  and  $A_3$ ) in this system will act and connected as counter electrodes if taking  $A_2$  as an example. And the build-in RE was connected to the reference electrode terminal.

## 3. Results and Discussion

### 3.1. Electrochemical behavior of sensor anodes

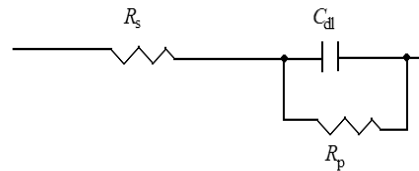


Fig. 3 - Equivalent circuit of the corrosion sensor embedded in the concrete / *Circuitul echivalent al senzorilor înglobați în beton.*

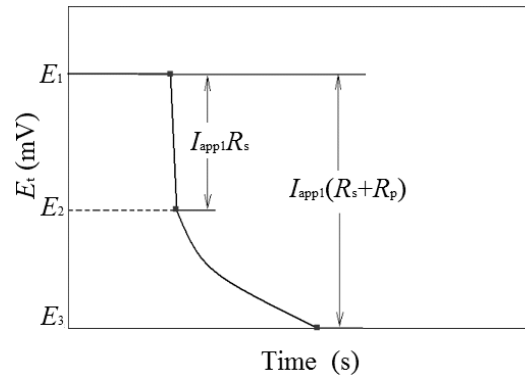


Fig. 4 - Typical polarization pattern of the CMS embedded in the concrete / *Model tipic de polarizare a CSM înglobat în beton.*

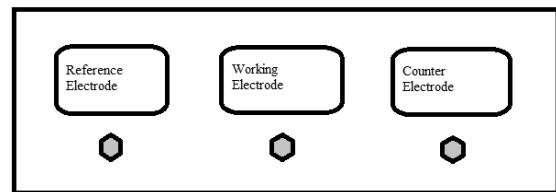
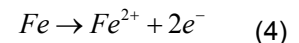
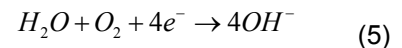


Fig. 5 - Cell configuration of the electrochemical station / *Configurația electrozilor în stația electrochimică.*

For the working steel anodes embedded in concrete, base on the pH of the concrete and the presence of aggressive ions (chloride sodium in this paper), the following would be the possible anodic reaction related to the anodes:



The possible cathodic reaction depends on the availability of  $O_2$  and on the pH near the working electrode surface. The most likely reaction is as follows:



Corrosion is the degradation of anodes by electrochemical reaction as shown in Equation (4) and (5). The chloride ions are not consumed by the electrochemical catalytic reactions but remains available for prolonged serious corrosion [9]. The open circuit potential (vs. Build-in RE) of the anodes have been transform to Standard potential (vs.  $Cu/CuSO_4$ ) in the concrete with different addition ratio of aggressive are given in Table 2. According to ASTM: C 876-91 [10], if the potentials

Table 2

Corrosion potential (vs. Cu/CuSO<sub>4</sub>) as a function of curing time for the sensors' anodes A2 and A5 in concrete containing 0, 0.3 and 3% Chloride, respectively.  
 Potentialul de coroziune (vs. Cu/CuSO<sub>4</sub>) a betonului conținând 0, 0,3 și 3% cloruri, funcție de timp pentru senzorii A2 și A5

| Chloride Addition / Adăosuri cloruri | A2   |      |      | A5   |      |      |
|--------------------------------------|------|------|------|------|------|------|
|                                      | 3d   | 7d   | 28d  | 3d   | 7d   | 28d  |
| 0%                                   | -9   | -13  | -14  | -10  | -15  | -15  |
| 0.3%                                 | -75  | -103 | -140 | -80  | -112 | -153 |
| 3%                                   | -130 | -311 | -455 | -142 | -344 | -519 |

of the anodes are more positive than -200 mV (vs. Cu/CuSO<sub>4</sub>) indicates a greater probability of the corrosion tendency. The control specimens and the specimens with 0.3% Chloride show most negative potential among the test period. The specimens with 3% chloride show some intermediate values of corrosion potentials at the first 7 days, but highest corrosion tendency after curing 28 days. The more negative potentials indicate greater corrosion tendency which is accompanied by greater pore fluid chloride concentrations and higher [Cl<sup>-</sup>]/[OH<sup>-</sup>] ratios in the concrete [11]. Usually after the sensor has detected the potential variation, the other units for measuring concrete resistance and polarization resistance began to work.

### 3.2. Concrete resistance and Polarization resistance

The plot of the the concrete resistance surrounded the sensor and the polarization resistance of the anodes with 0, 0.3 and 3% chloride addition have shown in Figure 6.

For concrete mix A, with no added chloride, was investigated as a reference concrete (or saying control specimen). It is shown in Figure 6(a) that the resistance is proportional to the chloride content. As expected, it was found that the concrete without adding chloride exhibited a very high resistance, above 3100 ohms. In contrast, a lower mortar resistance was measured in the concrete samples with 3% chloride in the mixture. Moreover, the addition of 0.3% chloride to the cement mortar produces a sharp decrease in the concrete resistance. A difference factor of more than 10 was observed when the resistance values of specimens C were compared to the values observed in specimen A. The decrease in mortar resistance with increasing chloride content can be explained by the chloride ion exchange interaction. Seen in this perspective, resistance variation provided a natural framework for the characterization of concrete properties analysis.

Figure 6 (b) shows that the polarization resistance values measured by the corrosion sensors in each concrete sample following a descending trend of A>B>C, and is similar to the trend of the electrical resistance values depicted in Figure 6 (a). The polarization resistance, R<sub>p</sub>, is commonly used as a measure of metal's resistance for corrosion damage. A high value of R<sub>p</sub> is associated with high ability of the corrosion

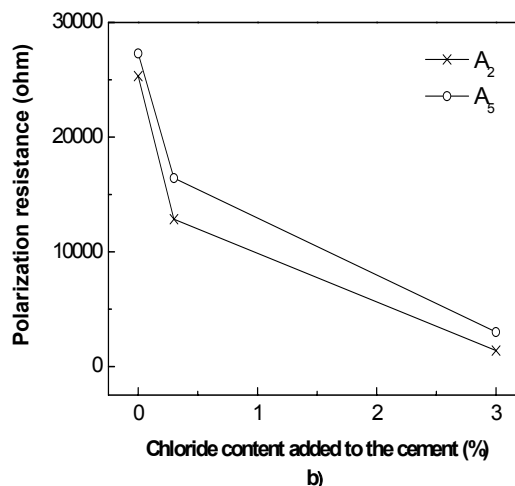
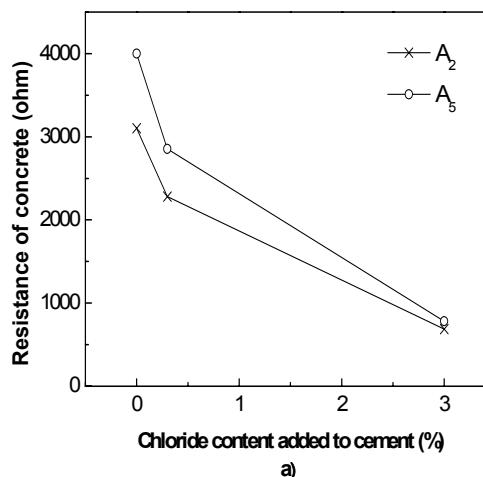


Fig. 6 - R<sub>s</sub> and R<sub>p</sub> values measured in the concrete A, B and C with different chloride contents / Valorile lui R<sub>s</sub> și R<sub>p</sub> măsurate în betoanele A, B și C având conținut diferit de cloruri.

prevention ; a low value of R<sub>p</sub> indicates high activity of the potential corrosion . Fig. 6 also shows that, in the absence of chloride contamination, R<sub>p</sub> increases as the concrete resistance increases. Generally, in this case, the corrosion rate is mainly controlled by the qualities of the concrete.

### 3.3. Regression coefficient

Alonso et al. have presented an empirical model depicts the relationship between the corrosion rate and concrete resistivity [9]:

$$i_{\text{corr}} = K / \rho_{\text{con}} \quad (6)$$

Where  $i_{corr}$  is corrosion rate of steel (in  $A/m^2$ ),  $K$  is regression coefficient (in  $V/m$ ), and  $\rho_{con}$  represents the concrete resistivity (in  $\Omega \cdot cm$ ). The equation (4) indirectly confirms that the concrete resistance directly influence and condition the corrosion and degradation rate of reinforcement concrete structures. In summary, the data developed in this study indicates that the electrical resistivity of concrete due to the chloride contamination in concrete is of concern as the key factors influenced the corrosion rate.

To obtain electrical resistivity of concrete, the geometric constant  $\alpha$  of the sensor(in  $cm$ ) is given as follows:

$$\alpha = R_s / \rho_{con} \quad (7)$$

Where  $R_s$  is resistance (in  $\Omega$ ), and  $\rho_{con}$  (in  $\Omega \cdot cm$ ) is concrete resistivity as mentioned above. The geometric constant of the sensor is calculated as:

$$\alpha = A/L \quad (8)$$

Where  $A$  is effective contact area (in  $cm^2$ ) of the concrete specimen ends,  $L$  is current path (in  $cm$ ) between two electrodes. For the sensor system with regular shape,  $A$  and  $L$  are easy to be measured. The value of  $\alpha$  for the present sensor should be calibrated in 0.01mol/L KCl solutions of known conductivity ( $0.0012737 S \cdot cm^{-1}$ ) are due to its complicated arrangements. The corrosion current  $i_{corr}$  can be calculated from  $R_p$  value using the Stern and Geary relationship, which is determined by the slope of the polarization curve in the vicinity of the corrosion potential:

$$i_{corr} = B/R_p \quad (9)$$

In general, the attempts to quantify the  $K$  have met both theoretical and empirical problems. A number of factors such as availability of oxygen, environment humidity, temperature and concentration of the ingressive ions, etc need to be taken into consideration before quantifying the  $K$ . However, this can be achieved by the new developed sensor. After  $i_{corr}$  has been defined by equation (9), a carefully analysis is carried out to determine the  $K$  value as shown in Table 3.

**Table 3**

K obtained from each sensor in the chloride-contaminated concrete  
*K obținut de la fiecare senzor din betonul contaminat cu cloruri*

| Chloride Addition<br><i>Adaosuri cloruri</i> | A2   | A5   |
|--|------|------|
| 0%   | 1.23 | 1.15 |
| 0.3%   | 1.04 | 0.91 |
| 3%   | 0.41 | 0.33 |

It should be noted that  $K$  value decreased with the increase of chloride addition ratio. The addition of 0.3% chloride has no visible influence on the  $K$  value, but the higher addition of chloride (3%) shows a lower  $K$  due to its high corrosion risk. One of the major advantages of this  $K$  evaluation is that it can be applied to classify the concrete using circumstance. Some improvements to the scheduling aspect of the  $K$  value may be brought through additional levels in the hierarchy for more detailed representation of the concrete quality.

#### 4. Conclusions

4.1 A novel CMS system that is suitable for embedding in chloride-contaminated concrete was developed for continuously monitoring the service condition of reinforced concrete structure. This system can provide the accurate measurement of electrical resistance of concrete, as well as polarization resistance of reinforced structure.

4.2 The testing data measured by CMS proved that the higher chloride ion content resulted in the lower electrical resistance of concrete and higher corrosion risk.

4.3 The electrical resistance of the concrete cover is proven to be another effective parameter for evaluating the corrosion risk of steel anodes, except for the polarisation resistance. The good quality sample of the concrete presented a value of  $R_s$  more than 2500  $\Omega$  while the mortar samples with added chloride presented values below 1000  $\Omega$ .

#### Acknowledgements

*This work is funded by the National Natural Science Foundation of China (No. 51108133) and China Postdoctoral Science Foundation (No. 20110491077). And this program is supported by National Key Technology R&D Program "Fabrication and Appliance of wall and roofing materials with multi-function include heat preservation and structure applied" (No. 2011BAE14B05).*

#### REFERENCES

1. S. Ahmad, Reinforcement corrosion in concrete structures, its monitoring and service life prediction-a review, *Cement and Concrete Composites*, 2003, **25**, 459.
2. W.J. McCarter, T.M. Chrisp, G. Starrs, P.A.M. Basheer, and J. Blewett, Field monitoring of electrical conductivity of cover-zone concrete, *Cement and Concrete Composites*, 2005, **27**, 809.
3. S.G. Millard, D. Law, J.H. Bungey, and J. Cairns, Environmental influences on linear polarisation corrosion rate measurement in reinforced concrete, *NDT&E International*, 2001, **34**, 409.
4. M.D. Newlands, M.R. Jones, S. Kandasami, and T.A. Harrion, Sensitivity of electrode contact solutions and contact pressure in assessing electrical resistivity of concrete. *Materials and Structures*, 2007, **41**, 621.
5. C.J. Newton, and J.M. Sykes, A galvanostatic pulse technique for investigation of steel corrosion in concrete, *Corrosion Science*, 1988, **28**, 1051.

6. H. Wojtas, Determination of Polarization Resistance of Reinforcement with a Sensorized Guard Ring: Analysis of Errors, *Corrosion*, 2004, **60**, 414.

7. R.Vedalakshmi, H. Dolli, and N. Palaniswamy, Embeddable corrosion rate-measuring sensor for assessing the corrosion risk of steel in concrete structures, *Structural control health monitoring*, 2009, **16**, 441.

8. S. Lu, Z. Wang, H.J. Ba, and Y.Z. Yang, Preparation of Ti/MnO<sub>2</sub> Reference Electrode and its Application in Concrete Structures, *Journal of Wuhan University of Technology-Mater. Sci. Ed.*, 2009, **24**, 161.

9. D. Whiting, Solving Rebar Corrosion Problems in Concrete, Paper No. 4, NACE, Houston, Tx, 1983

10. C. Alonso, C. Andrade, and J. A. Gonzalez, Relation between resistivity and corrosion rate of reinforcements in carbonated mortar made with several cement types, *Cement and Concrete Research*, 1988, **18**, 687.

11. R. Huang, J.Chang, and J. W. Correlation between corrosion potential and polarization resistance of rebar in concrete, *Material Letters*, 1996, **28**, 445.

\*\*\*\*\*

## MANIFESTĂRI ȘTIINȚIFICE / SCIENTIFIC EVENTS

### **12<sup>th</sup> International Conference on Ceramic Processing Science (ICCPs – 12) August 4-7, 2013, Portland, Oregon, USA**

ICCPs has evolved from a focus on particle-based processes to now including thin film processes, precursor approaches and all facets of the science underlying the basic themes of control and tailoring of ceramic-based materials with specific microstructure-property goals.

ICCPs-12 marks the 27<sup>th</sup> anniversary of the ceramic processing science series. Since 1986, the discipline has made significant progress in colloid and surface chemistry, powder synthesis, precursor-derived systems and sintering. However, much needs to be done to advance the scientific underpinnings of these processes, as well as the emergent areas of nanotechnology and its associated challenges, particle assembly, patterning, additive manufacturing, rapid sintering, and densification of complex shapes and multimaterial combinations.

ICCPs-12 will be comprised of plenary sessions in the morning and afternoon as well as concurrent sessions with both invited and contributed presentations. A poster session is also planned. Abstract submitting by February 6, 2013 in:

- Particle shape control and assembly
- Colloid dispersion and surface modification
- Rheology of concentrated suspensions
- Microfluidic techniques
- Patterning, templates, and self assembly
- Wet and dry shaping methods including additive manufacturing
- Solution and precursor thin film processes
- Reaction-based processes
- Biomimetic and bioinspired techniques
- Computational tools applied to processing
- Novel characterization and imaging tools
- Densification (nanoscale, multimaterial, complex shapes, novel approaches)
- Mesoscale, microscale and hierarchical manufacturing and design of microstructure
- Processes and processing designed to advance specific energy, electronic, optical and structural applications

**Contact:** <http://ceramics.org/meetings/12th-international-conference-on-ceramic-processing-science>

\*\*\*\*\*